JOURNAL OF GUIDANCE, CONTROL, AND DYNAMICS
Vol. 18, No. 3, May–June 1995

Spectral Analysis of Tethered Satellite System-Mission 1 Vibrations

S. Bergamaschi,* F. Bonon,† and M. Legnami†
University of Padova, Padova 35131, Italy

This paper presents part of the analysis of the frequencies of the free vibrations of TSS-1 (tethered satellite system-mission 1) in station-keeping conditions. As an evolution from previous work, a numerical-analytical model has been implemented for the study of tether-satellite coupled vibrations in the linear domain. The assumptions and main features of the model are briefly sketched, and its results are compared to the spectra obtained from the accelerometers mounted in the satellite. The acceleration data have been analyzed by means of two different methods, which have furnished power spectral densities in substantial agreement with each other and also with the most important theoretical expectations concerning tether transverse vibrations and satellite roll-pitch oscillations. Unfortunately, several concurring factors have, so far, precluded the determination of the fundamental mode of longitudinal tether vibrations.

Nomenclature

A	= tether cross section
d	= distance between tether attachment point and satellite c.o.m.
E	= tether material's Young modulus
I_1, I_2, I_3	= satellite principal moments of inertia
$\vartheta_1, \vartheta_2, \vartheta_3$	= satellite yaw, roll, and pitch angles, respectively
K	= satellite kinetic energy
l	= tether length
m	= satellite mass
n	= mean motion of the Shuttle orbit
s	= curvilinear coordinate along the tether
T	= tether tension
t	= time variable
(X, Y, Z)	= reference frame used for the data; in equilibrium conditions SLA-X is aligned to the orbital velocity and SLA-Z to the ascending local vertical
(x, y, z)	= orbital reference system used in the mathematical model, x along the ascending local vertical and z toward the orbit pole
α	= ratio between tether and satellite mass
β	= dimensionless wave number; longitudinal and transverse vibrations
μ	= tether mass per unit length
$'$	= space derivative

Introduction

THE tethered satellite system (TSS) is a joint program between the United States and Italy. After the signature of a Memorandum of Understanding in 1984, two of the scientific experiments selected for TSS-1, from the Smithsonian Astrophysical Observatory and from the University of Padova, were focused on the study of the dynamics of the system. The general work plan of both teams was to implement a number of mathematical models for the simulation of the dynamics, to analyze the data from the instruments onboard (in particular, from the accelerometers, gyros, and tensiometer) to compare theory results with data and, if necessary, to implement additional models. TSS-1 was flown in August 1992. Its mission profile was dramatically different from the nominal one, because only 257 m of tether could be unreeled, in contrast with the 20 km scheduled. Among the consequences, none of the electrodynamics primary objectives were performed and the active dynamics experiments, to take place during both the nominal stationkeeping phases, were ruled out.

In spite of this, it is the opinion of the authors that the scientific return of TSS-1, in terms of interest of the dynamics data collected, is significant. In fact, the duration of the real mission was close to nominal, so that, taking into account the predeployment checkout (PDC) phase after accelerometers and gyros calibration, about 55 h of scientific data could be recorded. In addition, the system was perturbed many times by satellite and Orbiter thrusters, so that several vibration modes were excited, with accelerations clearly detectable by the instruments onboard.

This feature is the basis of the present work, the purpose of which is the spectral analysis and interpretation of the satellite linear accelerometer (SLA) data, in partial fulfilment of the work plan already mentioned. More particularly, the bulk of what will follow is the presentation of the model being used for data interpretation, with particular emphasis for the justification of its simplifying assumptions, and the analysis of the data in the frequency domain, to identify the most important vibration modes and to compare measured with computed frequencies during the stationkeeping phases of the mission.

Mathematical Model

Since the model used for the interpretation of the data is an evolution of previous ones implemented by one of the authors, the main steps of the TSS dynamics analysis carried out at Padova University are briefly reviewed.

The first model taking into account tether elasticity was implemented in 1985.[1] Its main assumptions were: the motion is three dimensional; the Space Shuttle orbit is circular and unperturbed; the tether is a perfectly elastic unidimensional continuum and its length is constant; the satellite is a point mass; only the linear vibratory regime is considered. From the simulations, several conclusion could be made. 1) Gravity gradient dominates the two quasirigid libration modes, with frequencies very close to $n\sqrt{3}$ and $2n$, where n is the orbital mean motion. 2) Tether elasticity is by far the leading factor in the dynamics of the upper modes of lateral vibrations, where gravity gradient is important only because it provides the equilibrium tension; therefore, the frequencies of the upper modes of in-plane and out-of-plane transverse vibrations are almost coincident. 3) Longitudinal vibrations are scarcely affected by gravity gradient.

The main drawback of the model was that it took into account tension variations along the tether, so that the resulting system of partial differential equations was linear but with variable coefficients; therefore, the computation of eigenvalues and eigenfunctions

Received Nov. 4, 1993; revision received July 5, 1994; accepted for publication July 11, 1994.

*Associate Professor, Department of Mechanical Engineering, Via Venezia 1. Member AIAA.

†Research Assistant, Department of Mechanical Engineering, Via Venezia 1.

required the use of numerical methods for the solution of the final boundary value problem. To avoid the large number of computations required to simulate many systems with widely different characteristics (e.g., $0 < l < 20$ km), it was decided to try to take advantage of the fact that, for TSS-1 in nominal mission conditions, the tether mass was at most one-third of the satellite mass, so that the tension varies only slightly along it. If so, it is reasonable to replace the tension function in the equations with its average value and to obtain a set of equations with constant coefficients. This was presented in Ref. 2, where the other assumptions previously mentioned have not been changed. From the point of view of the computations involved, the simplification is dramatic; in fact, in Ref. 2 it is seen that the eigenvalue problem for each kind of vibration can be reduced to the solution of the transcendental algebraic equation

$$\beta * \tan \beta = \alpha \tag{1}$$

where α is the mass ratio $\mu l/m$. In addition, the comparison with the results of Ref. 1 showed that the relative errors in the frequency values introduced by the average were of the order of 0.1% even in the case with $l = 20$ km, where tether inertia and tension variability are at their maxima. It is noted that in the real TSS-1 mission, with a maximum deployed length of 257 m, the results are indistinguishable.

Another feature of the motion pointed out in Ref. 2 is that the coupling between longitudinal and transverse in-plane vibrations is weak, because of the large difference between the uncoupled frequencies. This fact, together with the smallness of the strain caused by gravity gradient, has suggested a comparison of the results of the averaged equations to the ones furnished by simpler models, where coupling is neglected and the tether is assumed to be inextensible. Again, in the worst case, i.e., when $l = 20$ km, the maximum relative error in the frequencies of the lateral modes was found to be 2.6%, so that string-like equations could be used for the harmonic analysis.

A limiting feature of both the models just mentioned is that the satellite is a point mass. The coupling between its attitude motion and tether lateral vibrations has been investigated in Ref. 3, where the satellite was assumed to be a rigid body and the conditions for the occurrence of internal resonances were studied in the planar case. The present model is mostly the result of the experience acquired from Refs. 1–3. It takes into account tether extensibility, three-dimensional lateral vibrations, and satellite rotations in the small oscillation amplitudes regime. This restriction does not appear to be excessively severe, because the present analysis is focused on stationkeeping conditions, when the tension, though small, did not vanish and exhibited, most of the time, only small high-frequency variations with respect to its average value.

The other main simplifying assumption is that the orbital reference system centered at the Shuttle end of the tether is considered to be inertial, so that the mean motion is zero in the derivation of the kinetic terms of the Lagrange equations. This simplification, apparently rather crude, seems to the authors to be justified by two considerations: 1) The frequencies of the really elastic modes of the tether are almost independent from the comparatively slow mean motion of the Shuttle. 2) The accelerometer data are sprinkled with short blank periods, so that the fast Fourier transform (FFT) analysis cannot be done with data spans longer than about 15 min. Of course, this circumstance precludes the possibility of straightforward detection of the slow components of the motion, as librations, which are directly affected by the mean motion.

Let us consider the reference system $(S, \boldsymbol{a}_1, \boldsymbol{a}_2, \boldsymbol{a}_3)$, shown in Fig. 1, with its origin at the Orbiter end of the tether, the x axis along the upper local vertical, y in the direction of the orbital velocity, and z parallel to the orbit pole. Let also $(G, \boldsymbol{e}_1, \boldsymbol{e}_2, \boldsymbol{e}_3)$ be the principal inertia system of the satellite which, in equilibrium conditions, is assumed to be parallel to the orbital frame. In this case, the radius vector to the satellite c.o.m. is

$$\boldsymbol{SG} = \boldsymbol{SP} + \boldsymbol{PG} = [l + x(l,t)]\boldsymbol{a}_1 + y(l,t)\boldsymbol{a}_2 + z(l,t)\boldsymbol{a}_3 + d\boldsymbol{e}_1 \tag{2}$$

where $x(l,t)$, $y(l,t)$, and $z(l,t)$ are the departure displacements from equilibrium of the satellite end of the tether, and d is the offset

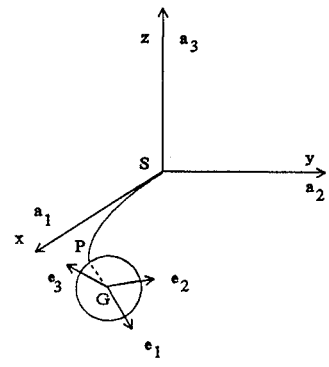

Fig. 1 Reference system.

between the tether attachment point and the satellite c.o.m. In the small angles approximation, the kinetic energy of the satellite can be written

$$K = \tfrac{1}{2}m\left[\dot{x}^2 + (\dot{y} + d\dot{\vartheta}_3)^2 + (\dot{z} - d\dot{\vartheta}_2)^2\right] + \tfrac{1}{2}\left(I_1\dot{\vartheta}_1^2 + I_2\dot{\vartheta}_2^2 + I_3\dot{\vartheta}_3^2\right) \tag{3}$$

where the convention for the angles is the same as in Ref. 4.

The forces on the satellite are as follows.

Gravity gradient, applied at the c.o.m.:

$$\boldsymbol{F}_1 = 3mn^2(l + x + d)\boldsymbol{a}_1 \tag{4}$$

To be precise, the m in Eq. (4) should be substituted by $m + \mu l/2$. In the TSS-1 mission, however, due to the short tether length and to lack of precise information about satellite fuel consumption, the distinction is more of academic than of practical relevance.

Taut tether reaction, applied at P and directed along the tangent to its terminal element:

$$\boldsymbol{F}_2 = -3mn^2(l + x + d)(\boldsymbol{a}_1 + y'\boldsymbol{a}_2 + z'\boldsymbol{a}_3) \tag{5}$$

where the quantity in the last parenthesis is the direction of the tangent to a point of a curve with small curvature.

Tether elastic reaction to longitudinal displacements, also applied at P:

$$\boldsymbol{F}_3 = -EAx'(\boldsymbol{a}_1 + y'\boldsymbol{a}_2 + z'\boldsymbol{a}_3) \tag{6}$$

If the Q_i are the generalized forces corresponding to $\boldsymbol{F}_1$, $\boldsymbol{F}_2$, and $\boldsymbol{F}_3$, writing the Lagrange equations in the form

$$\frac{\mathrm{d}}{\mathrm{d}t}\left(\frac{\partial T}{\partial \dot{q}_i}\right) - \frac{\partial T}{\partial q_i} = Q_i \qquad (i = 1, \ldots, 6) \tag{7}$$

after routine derivations and dropping mixed nonlinear terms, the following system is obtained:

$$\begin{gathered} \ddot{\vartheta}_1 = 0 \\ \left(I_2 + md^2\right)\ddot{\vartheta}_2 - md\ddot{z} + Td\vartheta_2 = 0 \\ \left(I_3 + md^2\right)\ddot{\vartheta}_3 + md\ddot{y} + Td\vartheta_3 = 0 \\ m\ddot{x} + EAx' = 0 \\ m\ddot{y} + md\ddot{\vartheta}_3 + Ty' = 0 \\ m\ddot{z} - md\ddot{\vartheta}_2 + Tz' = 0 \end{gathered} \tag{8}$$

where $T = 3mn^2(l + d)$ is the constant tether tension. The first of Eqs. (8) expresses the fact that yaw must be actively controlled, because the tether elastic torque on the satellite is negligible. From the other equations it is seen that roll is coupled to transverse out-of-plane vibrations and pitch to in-plane tether oscillations; further, longitudinal vibrations (in the x direction) are not coupled with the other degrees of freedom.

Table 1 SLA performance data

	X	Y	Z	Notes
Range, m-g	−20/ + 20	−20/ + 20	−20/ + 60	
Resolution, μ-g	0.61	0.61	1.22	
Meas. Bandwidth, Hz	4.7	4.7	4.7	−3 dB filtered
Sampling Period, ms	64	64	64	
Overall accuracy dc	3.9	11.6	12.5	at 10 m-g
RSS, μ-g	5.8	12.5	13.5	at 20 m-g
After 20.5 h thermal stabilization, base plate temperature 5–45°C	—	—	20.3	at 60 m-g
Overall accuracy ac	9.9	10.0	10.3	at 1 Hz, 10 m-g
RSS μ-g,	19.6	19.6	20.0	at 1 Hz, 20 m-g
After 20.5 h thermal stabilization, base plate temperature 5–45°C	—	—	59.1	at 1Hz, 60 m-g
Absolute bias, m-g	−0.198	−0.252	1.211	ground data
Bias trend, μ-g/h	0.05	0.37	0.41	ground data
After 20.5 h thermal stabilization				

System (8) admits, for each vibration mode, particular solutions having the form

$$\begin{aligned} x_n(s,t) &= a_n \sin(\beta_n s/l) q_n(t) \\ y_n(s,t) &= b_n \sin(\beta_n s/l) q_n(t) \\ z_n(s,t) &= c_n \sin(\beta_n s/l) q_n(t) \\ \vartheta_{2n}(t) &= \vartheta_{02} q_n(t) \\ \vartheta_{3n}(t) &= \vartheta_{03} q_n(t) \end{aligned} \tag{9}$$

where s is the independent space variable along the tether and the $q_n(t)$ are harmonic functions, the frequencies of which must be determined.

For longitudinal vibrations, β_n is the nth solution of Eq. (1), whereas

$$\omega_n = \frac{\beta_n}{l}\sqrt{\frac{EA}{\mu}} \tag{10}$$

In the case of each of the two partial coupled problems (transverse inplane and pitch, or transverse out of plane and roll) β_n is a solution of

$$\beta \cdot \tan\beta = \frac{\mu l}{m}\left(1 + \frac{md^2\beta^2}{I\beta^2 - \mu d l^2}\right) \tag{11}$$

which has been derived in Ref. 3 and where I is the proper moment of inertia.

Hardware Performance and Data Quality

The SLA has been provided by the Agenzia Spaziale Italiana, as part of the scientific core equipment of TSS-1. Its in-flight performance and operation have been discussed in Ref. 5, so that only a short overview is appropriate here.

The accelerometric package is made up by three pendulous accelerometers manufactured by Bell Aerospace TEXTRON, with sensitive axes along mutually orthogonal directions. The physical principle on which each sensor is based is the balance between the force acting on a proof mass and the restoring action generated by a coil. The motion of the mass is picked off capacitively, and the error signal is used to feed the balancing coil. This input is converted in a voltage reading proportional to the perturbing acceleration. The main characteristics of the instruments are summarized in Table 1.

An important inconsistency of the notation must be pointed out. It is caused by the fact that in all of the papers written on the argument (since years before the mission) the authors have always used the same attitude reference system, with x, in equilibrium conditions, parallel to the local vertical, and y and z in the horizontal plane; therefore, the notation of the mathematical model is coherent with previous works. Obviously enough, the frame (and associated rotation matrices) which was used to label the reference directions for the scientific data distributed to all the principal investigators of TSS-1 was different. This entails that, in the table and in the following, X is the direction of the sensitive axis of the instrument which, in equilibrium conditions, is aligned with the orbital velocity; Y is the nominal out-of-plane direction; and Z is along the local vertical. From the table it is seen that the range of SLA-Z differs from the others; this is because the steady-state gravity gradient acts in the nominal Z direction. It is also noted that the bandwidth is too narrow to detect the upper modes (if any) of longitudinal vibrations during the real mission. In fact, the bandwidth had been optimized before the mission in relation to the vibration spectrum expected in nominal stationkeeping conditions, with $l = 20$ km. Since most of the vibration frequencies are length dependent, the spectra at 257 m are displaced toward higher values. This is not a problem for transverse vibrations, which are comparatively slow; on the contrary, only the spring-mass mode of longitudinal oscillations, which are faster, is not cut out by the low-pass filter of the SLA.

The accelerometers have been calibrated both before and during the mission. The in-flight calibration consisted of three different time intervals of about 10 min (each) of continuous measurements, during which the Orbiter maneuvered to reach the inertial equilibrium attitude and then switched to free drift. The result has been that the bias and bias trend of SLA-X and SLA-Y were essentially comparable to the values measured before the mission; on the contrary, SLA-Z exhibited four kinds of anomalies: 1) absolute bias larger than the value measured on ground, 2) long term trend larger than measured on ground (same for SLA-Y), 3) step variations, not identified on ground, and 4) spikes, not present on ground.

The SLA data were acquired at the Science Operations Control Center in near real time by means of the software implemented at the South-west Research Institute (SwRI) and distributed to the TSS-1 principal investigators. The same software is used for playback visualization.

As already mentioned, an additional problem for the analysis of the data is the presence of blank periods, usually short, throughout the mission. To the knowledge of the authors, it is possible that the blanks are due to the data quality checks of the software which converted instruments readings in engineering units. The main impact on the spectral analysis is that it has not been possible to select time intervals longer than approximately 15 min during which the data flow from the three instruments was not interrupted; in turn, this means that the direct FFT of the data can not provide information about the long period components of the dynamics, such as the librations of the system. Moreover, the accuracy with which different acceleration components are detected decreases sensibly with the frequency. In fact, if T_0 is the time duration of the data sample being analyzed and T_1 is the period of one of the signal harmonic components, the fundamental frequency is $1/T_0$ and the error in the estimate of T_1 is

$$|\Delta T| \leq T_1^2/2T_0 \tag{12}$$

With $T_0 = 262$ s and $T_1 = 100$ s, the maximum error amounts to 19 s; with $T_1 = 30$ s, $|\Delta T|$ is decreased to less than 2 s. Therefore, the

presence of blanks in the data is likely to be the major error source in the analysis. In fact, the SLA sampling frequency (16 Hz) is considerable higher than the ones corresponding to the fundamental modes of the tether, so that the interesting portions at the high-frequency side of the spectra are relatively far from the Nyquist limit, and it is seen from Table 1 that the bias trend during relatively short ($\leq$900 s) intervals is quite acceptable.

Thus, the time windows selected for the analysis to follow are the ones with no data blanks in any of the instruments, no step variations and no spikes in the SLA-Z data, and no tether slackness.

Data Analysis and Results

The experimental values which will be presented in the following have been obtained analyzing many data slices in stationkeeping conditions. Since many spectra were available, the measured frequencies are the ones at which the sharpest spike reached its maximum height.

Since it is known[6] that the spectral resolution of the FFT is relatively poor if the input data span is not long with respect to the signal periods, it has been decided to analyze the SLA data, in different periods when l was constant, with two independent methods: the FFT and the maximum entropy method (MEM), or Burg algorithm. The results of three FFT subroutines available in the literature have been compared and substantial agreement has been found; at the end of the simulations, the one most frequently used has been subroutine FFTCC of the International Mathematical and Statistical Libraries (IMSL), because it does not require that the data number be an integer power of two. The MEM subroutine is the one found in Ref. 7, with only minor modifications. Several test runs and comparisons between the spectra obtained with the two methods showed that the frequencies of the most important peaks for which theoretical estimates are available matched well and that, in some cases, the MEM is less effective in detecting high-frequency spectral components. Thus, though all of the data have been analyzed with both of the methods, the power spectral densities (PSDs) obtained by means of the MEM are not reported, because no really new information has been extracted from them.

Figure 2 gives an example of how the data looks during one such time interval; the bias reported in Table 1 for SLA-X is clearly apparent. Figures 3–5 are the FFTs of 4096 data from the three instruments in a period of 262 s starting at Greenwich mean time (GMT) 218/01:35:40. During this period l was 166 m, as a result of the maneuvers performed in the attempt to solve the mechanical problem in the deployer mechanism; also, the satellite was in hold mode, so that yaw was maintained close to zero.

Table 2 Comparison between measured and theoretical values of the most important vibration modes of the system, I = 166 m

Mode	Measured period, s	Computed period, s
Pitch	131.2 ± 32.8	122.1 ± 4.0
Second transverse	52.5 ± 5.3	51.0 ± 1.7
Third transverse	26.2 ± 1.3	25.8 ± 0.8
Fourth transverse	17.5 ± 0.6	17.3 ± 0.6

The most prominent spikes in Figure 3 occur at both the sides of the spectrum. In the low-frequency band, the three major peaks, in order of increasing frequency and decreasing amplitude, are due to satellite pitch and to the second and third in-plane modes of tether transverse vibrations, respectively. (It is noted again that the Pirst libratory mode is not detectable, because of its exceedingly low frequency.) Also the fourth mode is visible, but its amplitude is sensibly smaller. The comparison between expected [from Eq. (11)] and measured periods is shown in Table 2. The values used in the simulations are $l = 166$ m, $m = 500$ kg, $I = 127\ \text{kg}*\text{m}^2$, $\mu = 8.2 * 10^{-3}$ kg/m, and $d = 0.755$ m.

In Table 2, the numerical values of the experimental errors have been derived using formula (12) as an equality, so that they are maximum errors. The uncertainties in the theoretical periods have been computed differentiating Eq. (11) and assuming that l and d are known exactly, so that the sources of error are in the approximate knowledge of m and μ. In fact, during the mission, the satellite mass decreased (quite non-nominally) from about 518 to 480 kg, whereas for μ different successive values have been provided to the investigator working group (IWG) in the course of the years.

Assuming $\Delta m = 20$ kg and $\Delta\mu = 2 * 10^{-4}$ kg/m, it is found for the maximum relative error of the nth period

$$\Delta T_n / T_n \approx 3.25 * 10^{-2} \tag{13}$$

The values are given to the first decimal figure, because this is the smallest order of magnitude of the computed errors. It is clearly seen that the blanks are the dominant source of uncertainty at low frequency, whereas the errors of computed and experimental values of the upper modes are comparable.

The other, relatively minor, spikes in the left part of the spectrum require further study, currently in progress. What can be said, at the moment, is that several corresponding frequencies can be expressed as combination tones of the fundamental modes given in Table 2, i.e., by a formula as $|p\omega_i \pm q\omega_j|$ with p and q being small integers. Therefore, an interpretation is that they are due to nonlinear couplings and reach detectable amplitudes because the SLA is not placed close to the tether attachment point. This possibility has been investigated in Ref. 8; from numerical simulations compared with experimental spectra it has been found that appreciable effects due to satellite attitude motion can be expected even if its amplitude is small. In other words, the SLA detects tether vibrations filtered by satellite rigid motion.

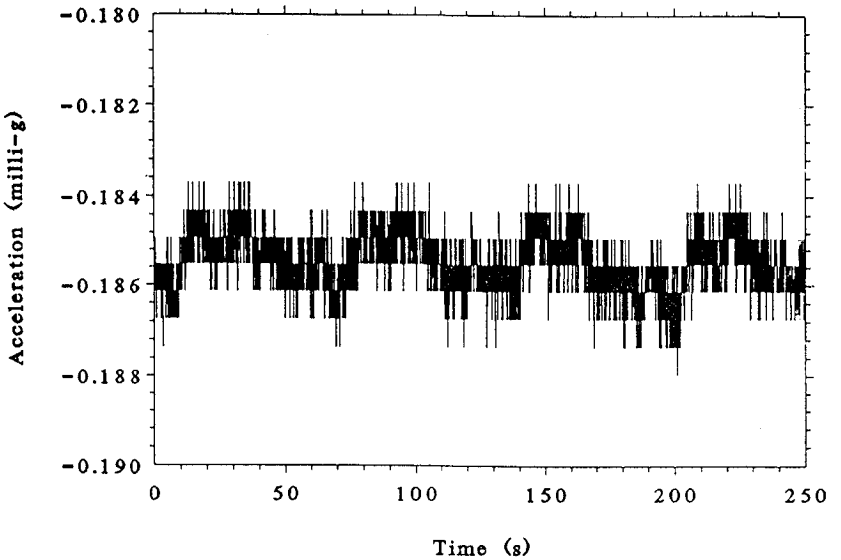

Fig. 2 SLA-X acceleration data vs time.

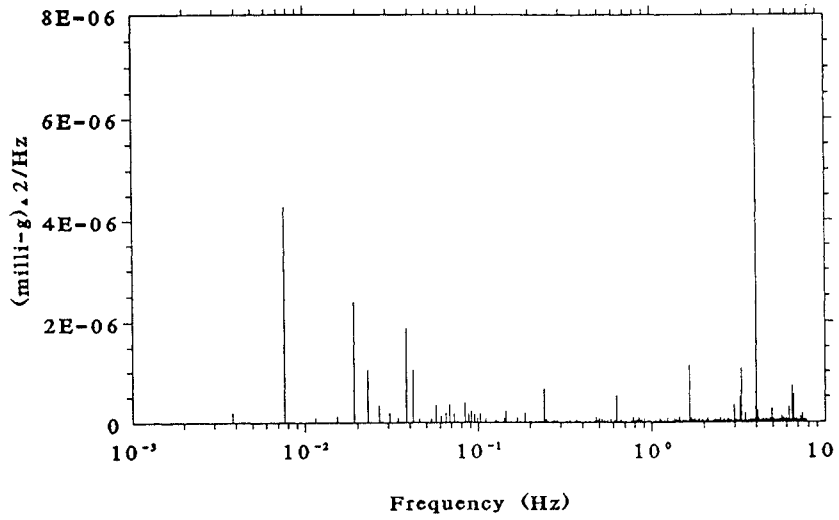

Fig. 3 Power spectral density of SLA-*X* data.

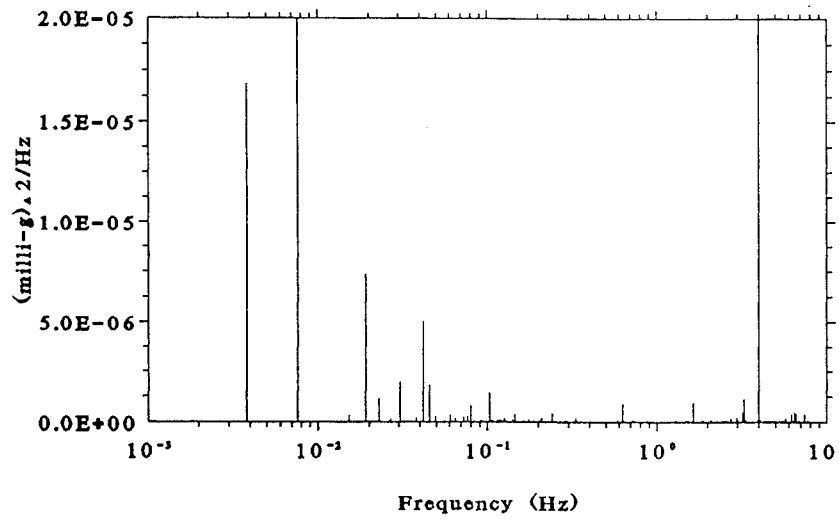

Fig. 4 PSD of fine SLA-*Y* data during the same time interval.

The high-frequency side (above 0.1 Hz) of the spectrum seems to be almost independent from the tether. In fact, it has been possible to compare the values measured by SLA-*X* with the theoretical structural analysis of the extended boom made by the staff of Martin Marietta. It turns out that the components at 0.23, 1.7, 3.9, and 6.4 Hz are close to the lower bending modes of the boom. In addition, it is known[9] that the first two modes of the Orbiter flexural vibrations, although payload dependent, are close to 3.3 and 5 Hz; both of these components can be seen in Fig. 3. The peak at 0.62 Hz is still unexplained; it is possible that it is generated by one of the vibration modes of the structure interfacing the boom and the Orbiter.

Figure 4 is the FFT of SLA-*Y* data in the same time window. The spike on the left has no physical meaning, because its frequency is exactly 1/262 Hz. The scale is not the same as used for SLA-*X* because the amplitudes are different, and otherwise some minor peaks would have disappeared. The differences with respect to Fig. 3 are relatively small, in the sense that the fundamental frequencies are the same, although some combination tones are different.

The spectrum of SLA-*Z* is interesting because, as expected from the simulations in Ref. 8, several peaks, which can be interpreted as combination tones with errors well within the ones given in Table 2, are apparent. If ω_1 is the roll/pitch frequency and the $\omega_i (i > 1)$ correspond to tether transverse modes, such tones include the lines at $1.2 * 10^{-2}(\omega_2 - \omega_1)$, $1.5 * 10^{-2}(2\omega_1)$, and 0.69 $(2\omega_3 - \omega_1)$ Hz as well as others, with minor amplitudes, generated by ω_3. Thus, nothing can be concluded about the spring-mass mode of longitudinal oscillations. During recent teleconferences about the reflight of TSS-1, Martin Marietta provided additional data about tether elasticity. According to these data, the Young modulus of the tether is a function of the tension, so that, at 166 m, tether EA is around 20,000 N. From other data of the SLA, it has been possible to make a first evaluation of tether elasticity and damping; in this way, it would seem that the value used earlier is slightly low. In any case, the frequency of the spring-mass mode would be between $8 * 10^{-2}$ and $9 * 10^{-2}$ Hz, which falls in a noisy part of the spectrum and is indistinguishable (if present) from other contribution.

Figures 6–8 are the FFTs of the data during the longest period (850 s) without blanks from any of the instruments. The fundamental features of the spectra are similar to those of previous ones; however, the following observations are made. 1) During this period the tether length was 257 m, so that the frequencies of the lateral modes are decreased in accordance with the theory. 2) Satellite pitch and roll are barely apparent in the figures, but from the tabular output of the PSD it is seen that their frequencies increased as expected. 3) A new component, with period close to 210 s, can be seen in all of the plots but, in particular, in Fig. 8 (because of the scale difference) where it causes the highest peak. Different interpretations are possible; they are not presented at this time because of the large uncertainty (±27 s) of the value. 4) Again, nothing can be said from Fig. 8

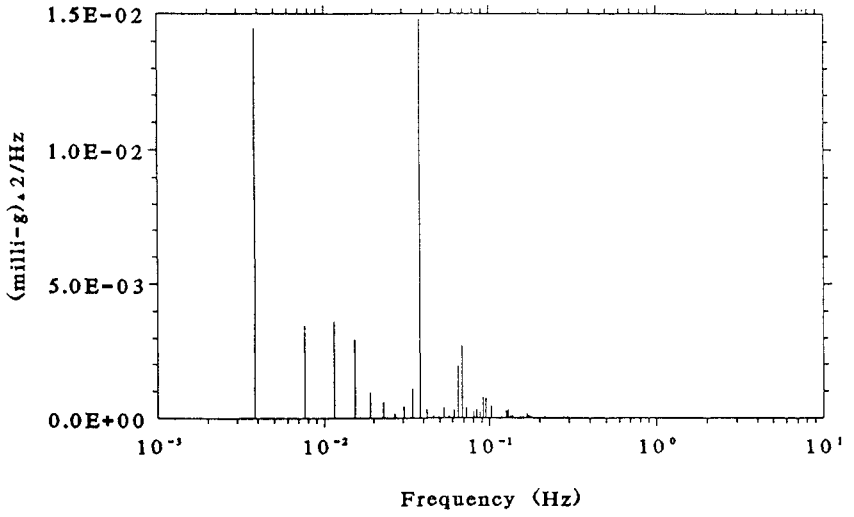

Fig. 5 PSD of fine SLA-Z data in the same interval.

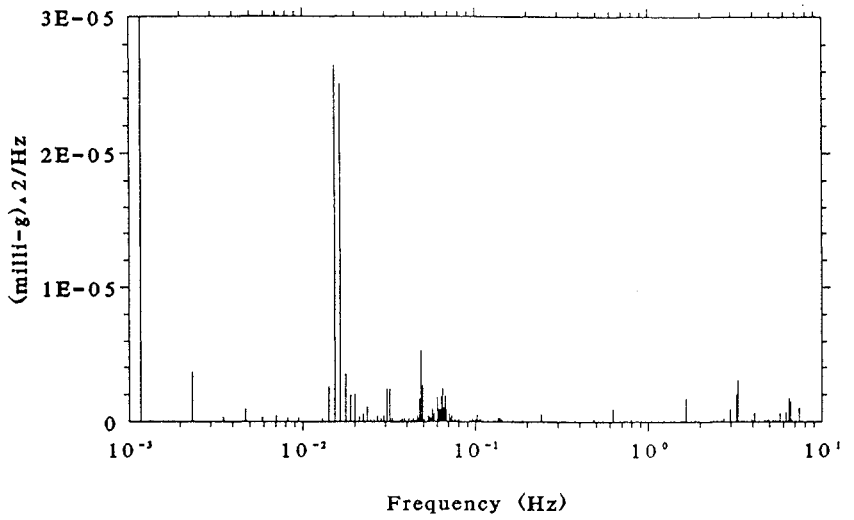

Fig. 6 PSD of SLA-X data with 13,281 points, tether length of 257 m.

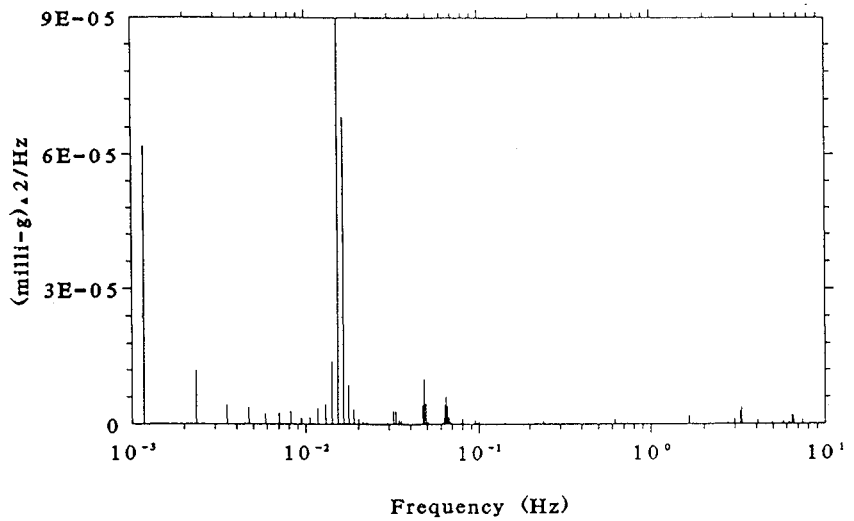

Fig. 7 PSD of SLA-Y data during the same interval of Fig. 6.

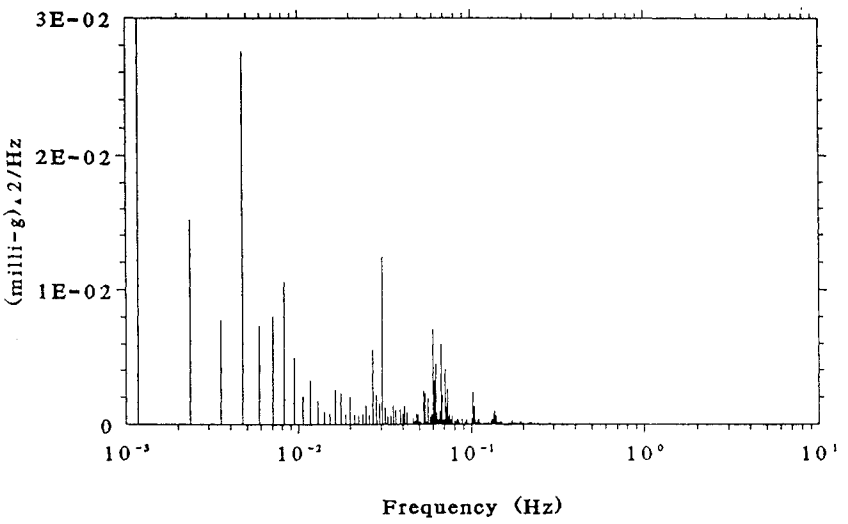

Fig. 8 PSD of SLA-Z data in the same interval of Fig. 8.

about the spring-mass mode which, perhaps, contributes to the spike around $7 * 10^{-2}$ Hz.

Conclusions

The work presented in this paper is the first part of an attempt to reconstruct and interpret the dynamics of TSS-1 from the analysis of all of the pertinent data; these include the output of the integrating gyros and the time histories of Orbiter attitude and satellite thrusters firings. It is the authors opinion that the quantity and quality (with the possible exception of SLA-Z) of data allow the statement that the dynamics experiments have not been spoiled significantly by the deployer problem, even if some DFOs have been cancelled. From the spectra examined so far, the following conclusions can be made.

1) The measured frequencies of the most characteristic components of the motion (transverse tether oscillations and satellite roll-pitch) match well with the expectations of the theory.

2) The spectra are somewhat denser than expected. The lower four modes of transverse vibrations and satellite roll-pitch are frequently present (also in different time intervals, not shown for sake of brevity) and, often, they generate combination tones with measurable amplitudes.

3) The sensitivity of the SLA is sufficient to detect accelerations from Orbiter-boom vibrations also in the deployed phase of the mission; in this respect, the damping properties of the short tether are poor.

4) The spring-mass mode is still unresolved and requires further study. As already mentioned, this is due to the concurrence of unfavorable circumstances, such as SLA-Z anomalous behavior, lack of precise information on tether EA, and position in the spectrum.

Acknowledgment

This work is part of the outcome of a research effort sponsored by Agenzia Spaziale Italiana under several contracts since 1984.

References

[1]Bergamaschi, S., Cusinato, S., and Sinopoli, A., "A Continuous Model for Tether Elastic Vibrations in TSS," AIAA 24th Aerospace Sciences Meeting, AIAA Paper 86-0087, Jan. 1986.

[2]Bergamaschi, S., and Catinaccio, A., "Further Developments in the Harmonic Analysis of TSS-1," *Journal of the Astronautical Sciences*, Vol. 40, No. 2, 1992, pp. 189–201.

[3]Bergamaschi, S., and Bonon, F., "Coupling of Tether Lateral Vibration and Subsatellite Attitude Motion," *Journal of Guidance, Control, and Dynamics*, Vol. 15, No. 5, 1992, pp. 1284–1286.

[4]Kaplan, M. H., *Modern Spacecraft Dynamics and Control,* John Wiley, New York, 1976, pp. 201, 202.

[5]Bergamaschi, S., Martino, M., Smargiassi, M., Musi, P., Meaney, M., and Steyn, J., "Evaluation of Pre-Deployment Dynamic Noise on TSS-1 during Mission STS-46," AAS/AIAA Astrodynamics Specialist Conf., Paper AAS 93-702, Victoria, BC, Canada, Aug. 1993.

[6]Kay, S. M., and Marple, S. L., Jr., "Spectrum Analysis—A Modern Perspective," *Proceedings of the Institute of Electrical and Electronics Engineers*, Vol. 69, No. 11, 1981, pp. 1380–1419.

[7]Press, W. H., Teukolsky, S. A., Vetterling, W. T., and Flannery, B. P., *Numerical Recipes,* Cambridge University Press, 1989, Chap. 12.

[8]Bergamaschi, S., Bonon, F., Merlina, P., and Morana, M., "Theoretical and Experimental Investigation of TSS-1 Dynamics," 44th Congress of the International Astronautical Federation, Paper IAF-93-A.3.21, Graz, Austria, Oct. 1993.

[9]Martin, G. L., Baugher, C. R., and Henderson F. H., "Early Summary Report of Mission Acceleration Measurements from STS-43," NASA Rept. Draft, Jan. 9, 1992.